Plasma Effects on Swirl Flames in a Scaled Dry Low Emission Burner

Liu, Xin; Subash, Arman Ahamed; Bao, Yupan; Li, Zhongshan; Ehn, Andreas; Hutig, Tomas; Larfeldt, Jenny ; Lörstad, Daniel; Nilsson, Thommie; Fureby, Christer

Published in:
AIAA Journal

DOI:
10.2514/1.J061050

2022

AIAA JOURNAL
Vol. 60, No. 6, June 2022

Plasma Effects on Swirl Flames in a Scaled Dry Low Emission Burner

Xin Liu,* Arman Ahamed Subash,† Yupan Bao,* Zhongshan Li,‡ and Andreas Ehn§
Lund University, 221 00 Lund, Sweden
Tomas Hurtig¶
Swedish Defense Research Agency, 164 40 Stockholm, Sweden
Jenny Larfeldt** and Daniel Lörstad††
Siemens Energy AB, 612 31 Finspång, Sweden
and
Thommie Nilsson‡‡ and Christer Fureby§§
Lund University, 221 00 Lund, Sweden

https://doi.org/10.2514/1.J061050

The effect of a rotating gliding arc (RGA) plasma discharge on the flame in a downscaled Siemens Energy dry low emission, SGT-750, burner was experimentally investigated under atmospheric combustion conditions. The central pilot section of the burner, named RPL (rich-pilot-lean), was redesigned with an integrated high-voltage electrode to generate an RGA. The exhaust gas was sampled and analyzed in terms of CO and NO_x emissions, and the CO emission data show that the RGA extends the lean blowout limit. High-speed OH chemiluminescence imaging was employed to understand the transient behavior of the flame in both conditions, with and without RGA, and also to study the process of flame restabilization by the assistance of the RGA. A flame kernel, initiated around the RGA channel, was observed to play an important role in the restabilizing process of the flame. Although the NO_x emission for the flame with RGA was found to be higher than that without RGA, it was still less than what previous data show for operating conditions with the RPL flame.

I. Introduction

THE need to achieve optimal performance of combustors in modern gas turbines necessitates low fuel consumption, high efficiency, low emissions, and stable combustion. The operation of lean premixed combustion in a modern gas turbine is a proven concept for maintaining a comparatively low flame temperature with the main purpose of reducing the production of thermal NO_x [1,2]. However, this lean operation may cause thermoacoustic instabilities, which in turn can result in unstable combustion with decreased combustion efficiency, local extinction, and flashback as direct consequences. This essential shortcoming is usually eliminated by adding a pilot diffusion flame that can stabilize the main flame, but an equivalent result can also be achieved by applying a plasma-assisted flame control system [3–6]. Implementation of a plasma-assisted flame control system in such a combustor can benefit the combustion process by decomposing larger hydrocarbon fuel molecules via thermal and kinetic effects, and enhancing the molecular transport. Such fuel-reforming concepts are advantageous because smaller fuel molecules can reach complete combustion faster and easier than larger hydrocarbons. High-energy electrons produce radicals and excited species through electron collisions, and therefore new reaction pathways are formed that can enhance the combustion process and extend the region in which the flame is stable [7–10]. Another potential advantage of using plasma-assisted flame control systems is the positive impact on the emission levels [11]. Various plasma methods have been developed and investigated to assist the combustion process, including microwave discharges [12,13], plasma jet/torch [14], gliding arc (GA) discharges [15,16], radio frequency discharges [17], nanosecond repetitively pulsed discharges [18], and many others. Among these, the GA discharge is regarded as a promising candidate for plasma-assisted combustion due to its high power density and straightforward deployment.

The characteristics of GA plasma and GA plasma-assisted combustion in either fundamental research burners or model gas turbine burners have previously been studied to some extent. Zhu et al. [19] conducted temperature measurements for a 35 kHz ac GA discharge and reported that the gas temperature of the GA is about 1100 K in an open electrode configuration (without swirling gas dynamics) at standard temperature and pressure. Lee et al. [9] studied the nonequilibrium characteristics of the rotating gliding arc (RGA). It was found that the plasma chemistry can be enhanced, and hydrogen selectivity can reach almost 100% by the RGA. Zhu et al. [20] investigated the effect of the airflow rates on the ground-state OH distributions with optical methods, and the results showed that the GA plasma is capable of generating a large amount of ground-state OH in the turbulent flow. A study on the stabilization mechanism of a turbulent flame by a filamentary plasma discharge by Kong et al. [21] showed that a turbulent jet flame can be sustained by a pin-to-pin GA discharge, in which the impact of GA plasma on combustion was mainly found as a thermal effect. The characteristics of GA plasma at different flow rates and its control effect on the static instability of the swirl flame have been studied by Chen et al. [22], which showed that the plasma may have acted as the ignition source that injected heat into the flame. In the work by He et al. [23], the effect of RGA on combustion efficiency in a swirling combustor was studied, and the combustion efficiency was found to be improved by the plasma-assisted combustion as compared with that in the normal conditions. Sun et al. [24] used air and methane in a

Presented as Paper 2021-0653 at the AIAA Scitech 2021 Forum, Virtual Event, 11–15 & 19–21 January 2021; received 10 September 2021; revision received 14 December 2021; accepted for publication 10 January 2022; published online Open Access 23 February 2022.

*Ph.D. Student, Division of Combustion Physics.
†Postdoctoral Researcher, Division of Combustion Physics.
‡Professor, Division of Combustion Physics.
§Senior Lecturer, Division of Combustion Physics.
¶Deputy Research Director, Defence and Security Systems and Technology.
**Senior Key Expert, Siemens Energy.
††Advisory Key Expert, Siemens Energy.
‡‡Postdoctoral Researcher, Department of Energy Sciences, Division of Heat Transfer.
§§Professor, Division of Heat Transfer, Department of Energy Sciences. Associate Fellow AIAA.

swirl burner with a cone-shaped bluff body to demonstrate an extension of the lean blowout limit by 38%. They also showed that this improvement can be even larger, up to 60%, for pulsating flames. One of the most important parameters in any experiment on plasma-assisted combustion is the ratio between the electrical power needed to significantly influence the flame and the thermal power of the combustion being assisted. In the work by Sun et al. [24] the ratio between electrical power and thermal power of the burner was 3%. Most previous work on swirl-stabilized gliding arcs have been conducted using specially designed laboratory burners; few studies have so far been reported on the effect of GA plasma-assisted combustion in an industrial gas turbine combustor. The investigation of plasma-assisted combustion on high-power facilities above 50 kW has only been studied using nanosecond pulsed discharges [25,26].

In the current work, a downscaled Siemens Energy dry low emission (DLE; SGT-750) burner was redesigned with integrated electrodes inside the original rich-pilot-lean (RPL) section of the burner to generate an RGA plasma discharge. The thermal power of the flames tested in this work was varied between 78 and 98 kW, and the RGA discharge generated here has an average power of 75–82 W, which is around 0.1% of the total thermal power. The electrodes were implemented inside the central pilot section, hereafter referred to as the RPL, which was designed to help stabilize the main and pilot flames [27]. Optical diagnostics, such as planar laser-induced fluorescence of OH and high-speed chemiluminescence imaging, have been applied to investigate the behavior of the main flame under the influence of RPL flame with different equivalence ratios at atmospheric pressure conditions [28,29]. Instead of the RPL flame as used in previous investigations, the RGA inside the RPL is only operated on air in the current setup. One objective was to keep as much as possible of the original design intact in order to enable quantitative comparisons between the behavior of the original burner and the modified version. Similar to the RPL flame, the RGA was found to be able to extend the stability region of the flame. In addition, the process of restabilizing a flame close to lean blowout (LBO) with the assistance of the RGA was studied by OH chemiluminescence. NO_x and CO emission monitoring was carried out and showed the LBO limit is pushed from $\Phi \leq 0.47$ to $\Phi \leq 0.45$ with the help of RGA while no significant increase of NO_x emission was detected. Optical emission spectroscopy was also performed approximately 2 cm above the burner throat (marked in Fig. 1) and the spectra was found much more pronounced with RGA on, indicating a much more intensive flame stimulated by the free electrons produced by the plasma.

II. Experimental Setup and Methods

To investigate the GA plasma-assisted combustion and analyze the effect of the GA plasma discharge on swirl-stabilized turbulent flames, a downscaled Siemens Energy DLE burner was employed. Various measurement methods were carried out, including high-speed OH chemiluminescence imaging, optical emission spectroscopy, and combustion emission sampling.

A. Burner Configuration

The configuration of the modified and downscaled Siemens Energy DLE burner is presented in Fig. 1a. The unmodified downscaled burner was designed by Siemens Energy AB for developing the engine of the SGT-750 gas turbine. A survey of the history of the development of the DLE burners and the principles that are involved can be found in Ref. [30]. It consists of three concentric stages: an outer section with a radial swirl, which is named Main; the intermediate section with an axial swirler, which is named Pilot; and the central body section called RPL [31]. Primarily, the RPL was designed to have its fuel–air feeds as well as a swirler, and to produce a premixed flame in it that can assist in stabilizing the main flame by supplying heat and chemically active species/radicals [32]. Following the standard operations, the fuel flow in the Pilot and Main sections can be regulated to control the local equivalence ratio independently. For the present experimental configuration, the bulk airflow velocity is set at 60 m/s [33,34] and the swirl number [35] is $S \sim 0.7$ [33,34] at the burner throat location. The airflow split between the Main and Pilot were 79% and 21%, respectively [33,34], which were determined from the pressure drop and effective area calculation [36] of the flow pathways. Downstream of the burner throat, there is a quartz conical frustum, here termed quarl, to smooth the flow. A rectilinear quartz combustor, being 40 cm in length and having a cross section of 10×10 cm^2 is mounted just downstream of the quarl to facilitate optical access. In the original burner design, a premixed flame was stabilized in the RPL section to help stabilize the main flame by supplying thermal energy and active radicals [32]. However, to generate a plasma discharge inside the burner in the current work, the RPL is modified to host an inner

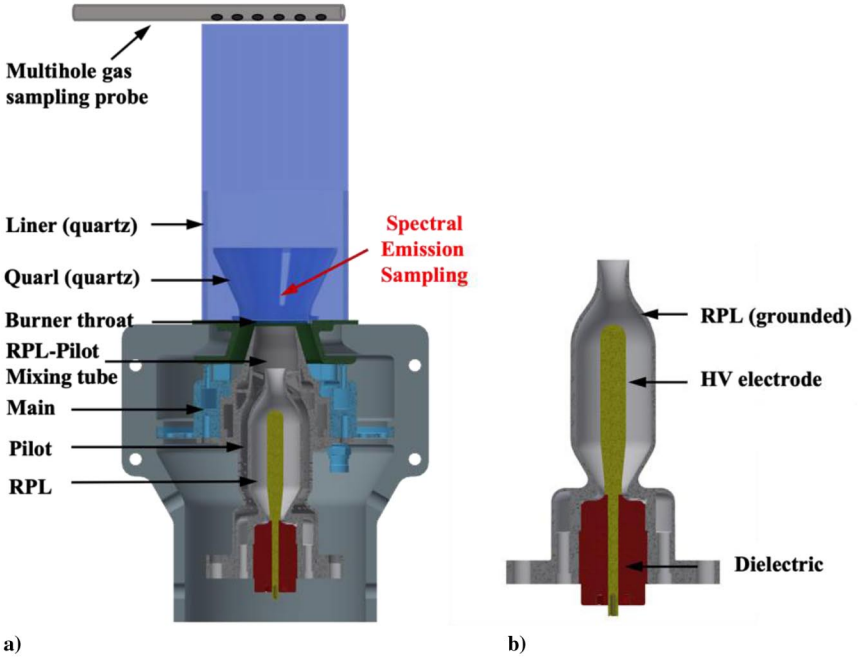

Fig. 1 a) Schematic of the downscaled and modified Siemens Energy DLE burner. b) The RPL section was modified with an inner HV electrode (yellow part).

high-voltage (HV) electrode (yellow part), as presented in Fig. 1b. All inner and outer dimensions of the RPL were kept unchanged, the injectors for fuel were removed, and at the base of the RPL [31] a dielectric insert was designed in order to galvanically separate the central electrode from the rest of the burner. Hence, the only geometrical change that can affect the flow patterns in the burner is the introduction of the 80-mm-long 12-mm-diameter electrode in the center of the RPL; see Fig. 1. One difference in the current work as compared to previous work, for example, Sun et al. [24], is that the discharge itself does not interact directly with the main flame, but instead it interacts with the pilot. With this configuration, stable operation conditions for the RGA can always be achieved by altering the parameters of RPL, for example, the temperature of the preheated gas, the flow rate, or the gas mixture composition. The HV electrode is connected to a 35 kHz ac power supply (Generator 9030 E, SOFTAL Electronic GmbH) and the outer shell of the RPL together with the remaining part of the burner is grounded. The characteristics of the GA discharge generated by this power supply are studied in detail in Ref. [37]. The voltage and current were monitored by a high-voltage probe (Tektronix 6015A) and a current monitor (Pearson Electronics, model 6585), and the instantaneous electrical power was calculated by taking the product of voltage and current, resulting in an average power of 75– 82 W, which is around 0.1% of the total thermal power. With the modified configuration, only air is fed through the RPL section.

B. Experimental Setup

A schematic of the experimental setup is presented in Fig. 2. The burner was installed vertically in an atmospheric combustion test rig at the Division of Combustion Physics at Lund University. The bulk airflow was provided by two blowers (Rietschle SAP 300), each of which had a maximum air mass flow of 55 g/s. Two thermal mass flow meters (Eldridge MPNH-8000, with accuracy $\pm 1\%$ reading and $\pm 0.5\%$ full scale) were mounted downstream of each blower to monitor the air mass flow. During the experiments, fluctuations up to 3% were observed in the flow rate. Every mass flow meter was followed by an inline heater (Leister) to provide a preheating temperature up to 750 K for the bulk air. The methane fuel used for both the Main and Pilot sections and the air supplied for the RPL were all controlled separately by mass flow controllers (Alicat Scientific MC-100SLPM, with accuracy $\pm 0.8\%$ reading and $\pm 0.2\%$ full scale).

As also presented in Fig. 2, a standard digital camera was used to take photographs of the flame. A high-speed complementary metal-oxide semiconductor (CMOS) camera (Phantom V7.1, Vision Research) equipped with a gated image-intensifier (Hamamatsu) was used to acquire the line-of-sight OH chemiluminescence images. The high-speed camera was equipped with a UV lens (UV-Nikkor, f/4.5, $f = 105$ mm) and a bandpass filter, centered around 310 nm, which targets OH^*. One thousand single-shot images were collected at 1 kHz framing speed for each flame condition and the exposure time was set to 50 μs. In addition, the spontaneous emission from the flame was measured by a fiber spectrometer (AvaSpec-ULS2048XL-EVO-RS-UA) with a broad spectral sensitivity range between 200 and 1160 nm. The gate of the spectrometer was set to 500 ms. Furthermore, a water-cooled multihole gas sample probe (PSP4000-H/C) with a sampling rate of 1 Hz was employed to enable an analysis of the combustion exhaust emission. The probe was arranged at the exit of the combustor liner to collect the combustion emission gas. The sample gas was then passed through a condenser to remove the water. The emission analysis system was calibrated by standard calibration gas bottles every day before measurements. The measurement ranges of the NO_x analyzer (Eco Physics model CLD822Mhr, by which the sum of NO and NO_2 can be acquired) and CO analyzer (Fuji Electric model ZKJ) are 50 and 2000 ppm, respectively (with accuracy $\sim \pm 1\%$).

During the experiment, the equivalence ratio at each section was altered by changing only the fuel amount while keeping the airflow constant. The equivalence ratio was gradually reduced until the LBO event occurred. The approximate critical values (for LBO) were approached by small changes ($\Delta\Phi = 0.01$) and by waiting at least 1–2 min at each setting to detect more accurate values of the critical equivalence ratios and stable emission results. The plasma discharge was controlled systematically on/off as changing the Φ, which always shows identical results.

C. RGA Channel Generated in the Burner

Figure 3 shows a schematic and a photograph taken from above with a standard single-lens reflex camera, of the downscaled Siemens Energy DLE burner, during plasma discharge without combustion. From the schematic, the Pilot and Main swirlers can be easily identified for reference. The discharge channel generated in the burner is initiated at the narrowest gap between the grounded RPL and the high-voltage electrode and afterward, and follows the swirling flow up to the top of the electrode. From Fig. 3b, it can be seen that the discharge channel is oriented along with the flow and rotated following the swirling motion in an anticlockwise direction generated by the swirlers in the Pilot. Each dot on the inner surface and the rim of the RPL nozzle is a cathode spot, and because the driving frequency is 35 kHz, each cathode spot is separated in time by 29 μs.

From previous experiments, it was observed that too-high flow rates easily trigger re-ignition of the gliding arc [20,37]. To avoid these events from occurring, the air injected into the RPL in the current work has been optimized by testing different mass flows

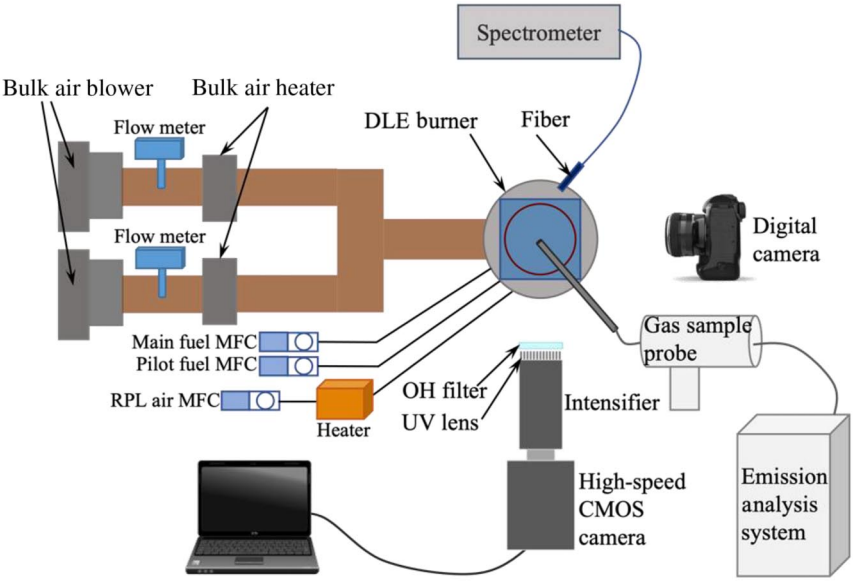

Fig. 2 Schematic of the experimental setup (MFC = mass flow controller).

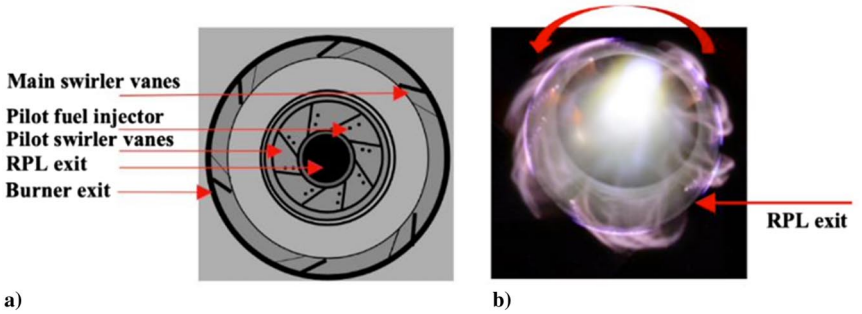

Fig. 3 a) Top view of the scaled Siemens Energy DLE burner showing Pilot and Main swirlers. b) Photograph of discharge using a standard digital camera. At atmospheric pressure and 300 K airflow, the discharge follows the swirling motion.

and preheating temperatures. The optimal flow condition, where these current measurements were conducted, was determined to be 0.35 g/s in terms of the air mass flow with a preheating temperature of 673 K.

III. Results and Discussion

A. Effect of RGA on Stabilizing the Flame

The flame stabilization mechanism for the reference operating conditions of this combustor, that is, when using the RPL flame but no plasma discharge, is well described in [29,33,38,39]. These previous results show that the interactions between the RPL flame and the more downstream located Pilot and Main flames play an important role in the overall flame stabilization. Moreover, these results show that the RPL flame, especially at rich conditions, contributes significantly to the overall flame stabilization. Here, the flame is anchored inside the quarl and is stabilized by a central recirculation zone (CRZ) in the combustor induced by a precessing vortex breakdown. Additional outer recirculation zones can also be observed at the junction between the quarl and combustor section.

In the prestudy for the current work, the downscaled Siemens Energy DLE burner, which has the same Pilot and Main flames (at equivalence ratio $\Phi = 0.47$), was tested with and without RPL flame ($\Phi = 1.2$) to compare the flame topology. For the case with the $\Phi = 1.2$ RPL flame, while keeping both Pilot and Main flames with $\Phi = 0.47$, the global equivalence ratio turns to be richer as $\Phi = 0.5$. The photographs of these two flames are presented in Fig. 4a, which confirms that the RPL flame helps to stabilize the main flame approaching LBO and to reattach the flame inside the quarl. In the current study, the RPL flame is replaced by the plasma discharge. The images of two flames at the same global $\Phi = 0.47$, without and with plasma discharge, are shown in Fig. 4b for comparison. The plasma discharge seems to be able to stabilize the main flame close to LBO, which also is achievable with the RPL flame. The RPL flame adds heat and chemically active species and radicals to the main flame that then can be stabilized. When the RPL flame is replaced by the RGA plasma, a similar stabilization effect to the main flame is presented by the plasma discharge, which can generate large amounts of reactive species and certain thermal energy for assisting combustion.

When the flame is close to the LBO limit, the flame temperature is sufficiently low, and high concentration of CO is produced in the combustion process due to the lower oxidation rates and incomplete combustion of hydrocarbon fuel [40]. So, the LBO limit can be determined by the exponential increase of CO emission and quantified by the CO emission value over 200 ppmvd, which showed consistent results. As shown in Fig. 5, for the flame without RGA in the RPL, the LBO limit can be identified at global $\Phi \leq 0.47$ by a dramatic increase in the CO emission, whereas for the flame with RGA in RPL, the LBO limit can be identified at global $\Phi \leq 0.45$. Figure 5 presents that the plasma discharge can extend the LBO limit of the flame, resulting from active radicals and the thermal energy generated along with the plasma channel, which can help sustain the flame.

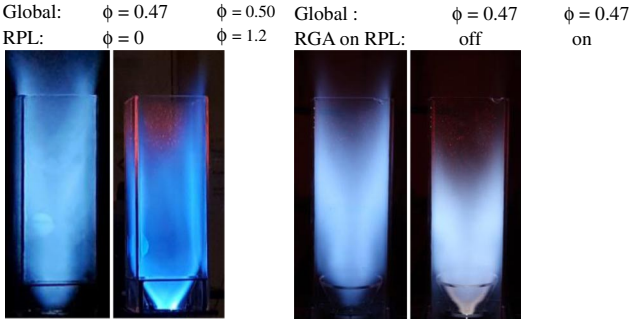

Fig. 4 Photographs taken with the standard digital camera is showing the total extension of the flame: a) without/with RPL flames, and b) without/with RGA, in which only air was injected in the RPL instead.

B. Effect of RGA on NO_x Emission

The effect of plasma discharge on the NO_x emission at various global equivalence ratios Φ is shown in Fig. 6. It can be observed that the NO_x is kept almost constant with the minimum level for the flames without RGA. However, with RGA on, the NO_x emission slightly changes with Φ, but the average level of NO_x production increases visibly. The increase in NO_x emission for operating with RGA can be a combination of the NO_x produced by the plasma when it 1) interacts with the air, and 2) initiates diffusionlike flame just after the RPL exit. Previous studies have already identified vibrationally excited nitrogen $[N_2(v)^*]$ and atomic oxygen (O) as the main sources of NO_x production when a gliding arc is interacting with the air [41]. As the fuel injections in the pilot vanes (see Fig. 3a) are quite close to the RPL exit, the pilot fuel and air do not get enough distance to achieve proper mixing before interacting with the discharge channel just after the RPL exit. A diffusionlike flame is initiated by this plasma channel, named a flame kernel, which contributes to NO_x increase through the thermal NO_x pathway. In addition, the flame becomes more compact with plasma stabilization, which increases the residence time for combustion products that generate more thermal NO_x. For the reference cases with RPL rich ($\Phi = 1.2$) flame in this burner [42], the RPL primary combustion is initiated inside the RPL section, and the fuel-rich exhausts initiate the secondary combustion after the RPL exit while interacting with the pilot fuel/air mixture before achieving a higher degree of mixing. This combustion is also initiated in a diffusionlike manner that contributes to the NO_x emission through the thermal NO_x pathway. The NO_x emission for the reference operating condition of the burner with RPL flame of $\Phi = 1.2$ {data reported in [42]} is also presented in Fig. 6 to compare with the results from current studies. It shows that although the level of NO_x production is higher for the flame with RGA than that without RGA, it is still less than that from the reference operation cases.

C. Process of RGA-Assisted Stabilization

The process of restabilizing a close-to-LBO flame by RGA assistance is illustrated in Fig. 7, in which single-shot images of OH

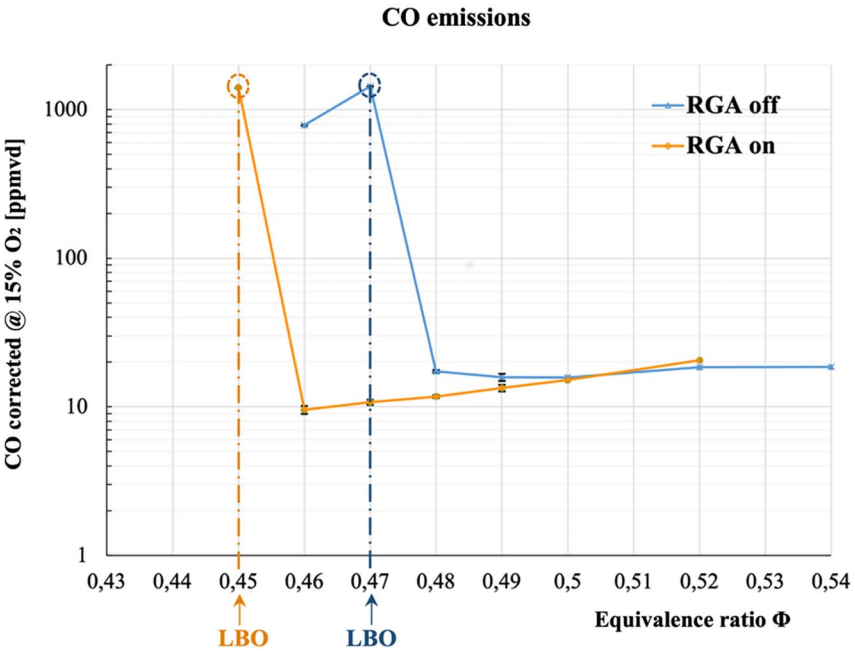

Fig. 5 LBO limits of the burner with/without RGA in RPL identified by CO emission level.

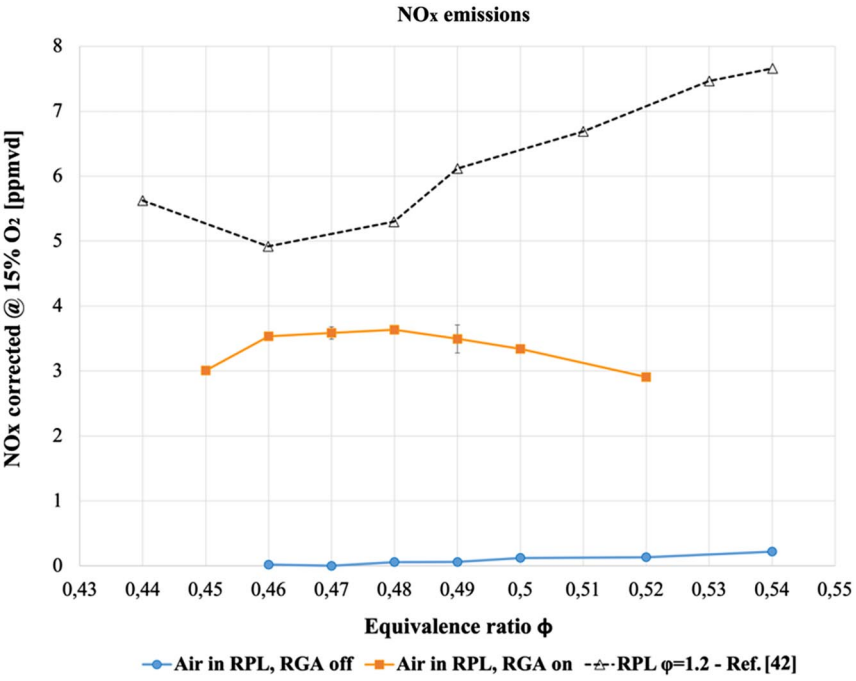

Fig. 6 Comparison of the NO_x emission levels between cases. Blue line: only air in RPL, orange line: air in RPL with RGA on, and dotted black line: with RPL flames that data are taken from {"NO_x (with Quarl) Global Change" in Fig. 3 of the Ref. [42]}.

chemiluminescence are presented as a time sequence over 23 ms. Before t_0, the flame was operated at an equivalence ratio just above LBO, and the equivalence ratio was decreased to $\Phi = 0.47$ at t_0, at which LBO starts to occur. In the time interval from t_0 to $t_0 + 2$ ms, the flame detaches and is about to blow out because it no longer anchors in the CRZ and hence the flame stabilization is lost. More specifically, the flame is observed to move up and away from the burner exit in a narrow shape following the helical motion of the flow exiting the burner nozzle. The RGA is switched on at $t_0 + 2$ ms, and as long as the RGA is applied a flame kernel is initiated by the plasma discharge when interacting with the pilot fuel/air. Plasma emission is not observed above the burner throat, hence, the plasma is not sustained in the flame kernel as it reaches the quarl. As shown in Fig. 7, the flame kernel started to influence and restabilize the unstable flame from $t_0 + 3$ ms. It takes around 9 ms to rebuild the CRZ in the flame, by which the flame can stabilize inside the quarl again. After the flame is completely stabilized with RGA assistance, the flame rotating with a helical motion is observed starting from $t_0 + 12$ ms. The period for this rotation is around 12 ms, which is equivalent to an 83 Hz frequency.

D. Flame Emission Spectra

Average spectra from 100 measurements for four cases with global $\Phi = 0.48$ and 0.52 with and without plasma discharge are shown in

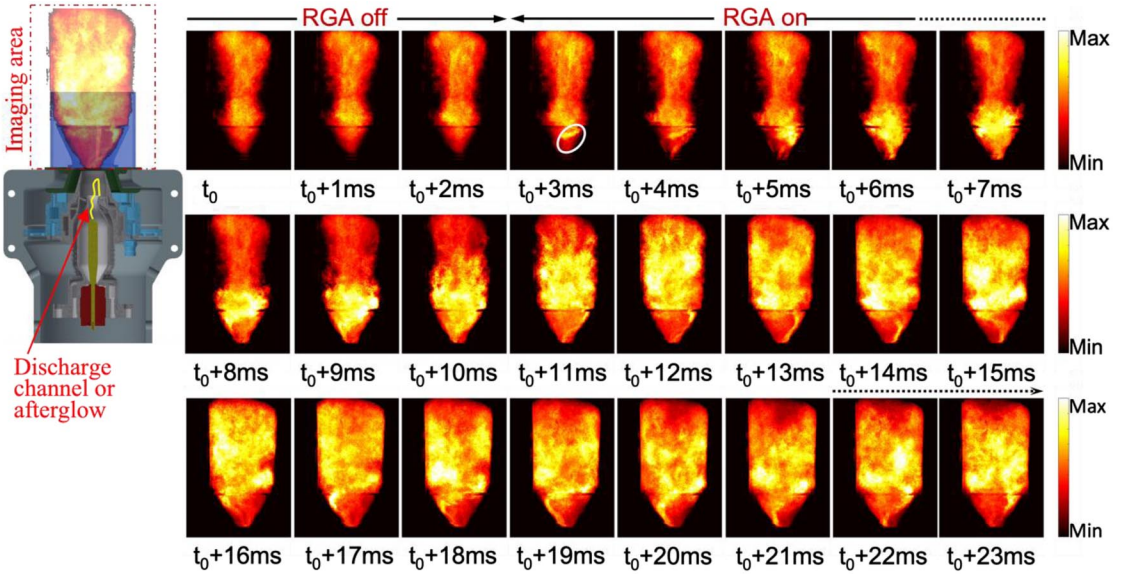

Fig. 7 OH chemiluminescence images showing the process of restabilizing a close-to-LBO flame at global equivalence ratios, $\phi = 0.47$, with RGA assistance.

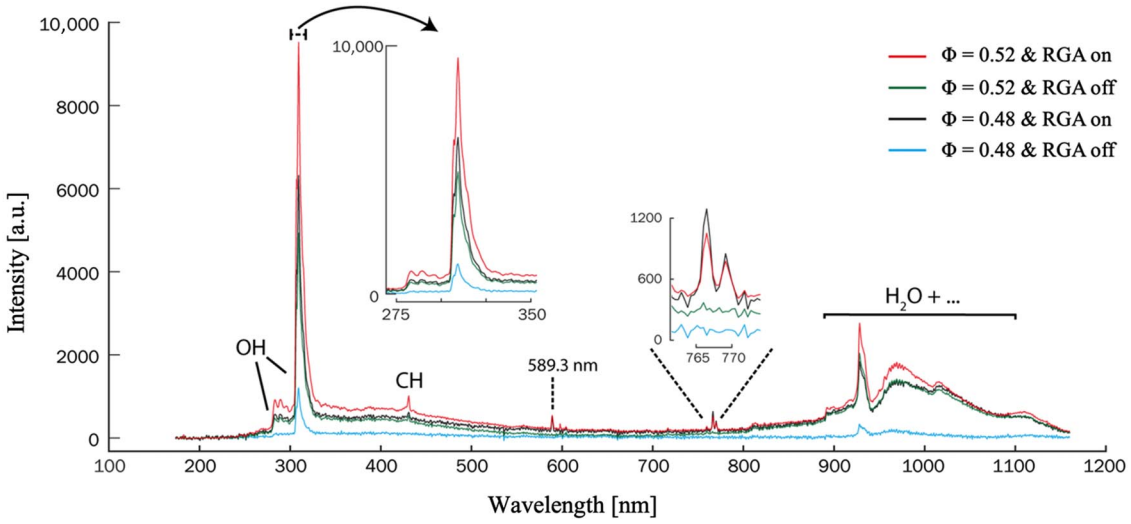

Fig. 8 The spectra of flames at global $\Phi = 0.48$ and 0.52 with/without RGA.

Fig. 8. It can be seen that all peaks are enhanced with increasing Φ. When the RGA is turned on, a large number of free electrons are produced, which will interact with ambient species and create ionized and/or excited molecules/atoms. As a result, the flame emission gets more intense, where all peaks are approximately 2–5 times stronger compared with the spectrum of the flame without RGA. In addition, more peaks show up when the RGA is turned on: the CH (A-X) peak around 430 nm and two relatively strong peaks at 590 and 767 nm. The first one has the wavelength of sodium D-lines (3p–3s), whereas the latter one coincides with the transition of excited potassium D-lines (4p–4s). The traces from Na and K are most likely contaminations in the plasma/burner setup, either in the high voltage electrode or the RPL nozzle, where the surface temperature is increased when the gliding arc is operating. Even though the amounts might be low, atoms are capable of producing strong atomic emissions. Moreover, unlike emission from radicals such as OH and CH, the intensity of the Na and K peaks is independent of the equivalence ratio. This behavior further supports that the Na and K peaks are not from the flame but are rather a sign of material ablation. Minor erosion (4 mm^3) of the electrode has been noticed after 100–200 h of operation.

IV. Conclusions

A downscaled premixed Siemens Energy industrial gas turbine burner, SGT-750, was equipped with an HV electrode in the RPL section and was tested under atmospheric conditions to investigate the effect of plasma discharge on the swirl flames. Several measurements were employed: high-speed OH chemiluminescence imaging, optical emission spectroscopy, and flame emission exhaust sampling analysis. The results of the current work indicate that the RGA plasma discharge plays a significant role in flame stabilization and extending the LBO limit. The restabilization process of a flame close-to-LBO by the RGA plasma is demonstrated by the OH chemiluminescence images in time sequence. A flame kernel initiated by the plasma discharge is observed to interact with and help stabilize the flame, resulting from the thermal energy and active chemical radicals generated by the plasma. Spectroscopic analysis shows clear emission peaks from Na and K when the RGA is turned on, indicating that the plasma is causing electrode wear during operation. Exhaust gas analysis shows that the NO_x emission for the flame with RGA is higher than that without RGA but still less than the reference case with RPL flame. All in all, these results show that an integrated RGA

system is capable of controlling the flame either by stable or transient operation without substantial NO_x emission.

Acknowledgments

This work has been financed by the Swedish Research Council (2021-04506) and the Swedish Energy Agency through the Centre for Combustion Science and Technology (CECOST) (38913-2) and the efficient electric combustion technology (EFFECT) II project (42555-1) as well as European Research Council (ERC) (669466, 852394). In addition, Xin Liu would like to thank the financial support from the China Scholarship Council.

References

[1] Warnatz, J., Maas, U., and Dibble, R. W., *Combustion*, 4th ed., Springer-Verlag, Berlin, 2006, pp. 237–253. https://doi.org/10.1007/978-3-540-45363-5

[2] Michaud, M. G., Westmoreland, P. R., and Feitelberg, A. S., "Chemical Mechanisms of NOx Formation for Gas Turbine Conditions," *Symposium (International) on Combustion*, Vol. 24, No. 1, 1992, pp. 879–887. https://doi.org/10.1016/S0082-0784(06)80105-0

[3] Matveev, I. B., Matveeva, S. A., Kirchuk, E. Y., Serbin, S. I., and Bazarov, V. G., "Plasma Fuel Nozzle as a Prospective Way to Plasma-Assisted Combustion," *IEEE Transactions on Plasma Science*, Vol. 38, No. 12, 2010, pp. 3313–3318. https://doi.org/10.1109/TPS.2010.2063716

[4] Matveev, I. B., Serbin, S. I., and Lux, S. M., "Efficiency of a Hybrid-Type Plasma-Assisted Fuel Reformation System," *IEEE Transactions on Plasma Science*, Vol. 36, No. 6, 2008, pp. 2940–2946. https://doi.org/10.1109/TPS.2008.2006843

[5] Korolev, Y. D., and Matveev, I. B., "Nonsteady-State Processes in a Plasma Pilot for Ignition and Flame Control," *IEEE Transactions on Plasma Science*, Vol. 34, No. 6, 2006, pp. 2507–2513. https://doi.org/10.1109/TPS.2006.884791

[6] Korolev, Y. D., Frants, O. B., Landl, N. V., Geyman, V. G., Shemyakin, I. A., Enenko, A., and Matveev, I. B., "Plasma-Assisted Combustion System Based on Nonsteady-State Gas-Discharge Plasma Torch," *IEEE Transactions on Plasma Science*, Vol. 37, No. 12, 2009, pp. 2314–2320. https://doi.org/10.1109/TPS.2009.2034163

[7] Ombrello, T., Qin, X., Ju, Y., Gutsol, A., Fridman, A., and Carter, C., "Combustion Enhancement via Stabilized Piecewise Nonequilibrium Gliding Arc Plasma Discharge," *AIAA Journal*, Vol. 44, No. 1, Jan. 2006, pp. 142–150. https://doi.org/10.2514/1.17018

[8] Ombrello, T., Ju, Y., and Fridman, A., "Kinetic Ignition Enhancement of Diffusion Flames by Nonequilibrium Magnetic Gliding Arc Plasma," *AIAA Journal*, Vol. 46, No. 10, Oct. 2008, pp. 2424–2433. https://doi.org/10.2514/1.33005

[9] Lee, D. H., Kim, K. T., Cha, M. S., and Song, Y. H., "Optimization Scheme of a Rotating Gliding Arc Reactor for Partial Oxidation of Methane," *Proceedings of the Combustion Institute*, Vol. 31, No. 2, Jan. 2007, pp. 3343–3351. https://doi.org/10.1016/j.proci.2006.07.230

[10] Feng, R., Li, J., Wu, Y., Jia, M., and Jin, D., "Ignition and Blow-Off Process Assisted by the Rotating Gliding Arc Plasma in a Swirl Combustor," *Aerospace Science and Technology*, Vol. 99, April 2020, Paper 105752. https://doi.org/10.1016/j.ast.2020.105752

[11] Serbin, S. I., Matveev, I. B., and Mostipanenko, G. B., "Investigations of the Working Process in a "Lean-Burn" Gas Turbine Combustor with Plasma Assistance," *IEEE Transactions on Plasma Science*, Vol. 39, No. 12, Dec. 2011, pp. 3331–3335. https://doi.org/10.1109/TPS.2011.2166811

[12] Ehn, A., Petersson, P., Zhu, J. J., Li, Z. S., Aldén, M., Nilsson, E. J. K., Larfeldt, J., Larsson, A., Hurtig, T., Zettervall, N., and Fureby, C., "Investigations of Microwave Stimulation of a Turbulent Low-Swirl Flame," *Proceedings of the Combustion Institute*, Vol. 36, No. 3, 2017, pp. 4121–4128. https://doi.org/10.1016/j.proci.2016.06.164

[13] Rao, X., Hemawan, K., Wichman, I., Carter, C., Grotjohn, T., Asmussen, J., and Lee, T., "Combustion Dynamics for Energetically Enhanced Flames Using Direct Microwave Energy Coupling," *Proceedings of the Combustion Institute*, Vol. 33, No. 2, 2011, pp. 3233–3240. https://doi.org/10.1016/j.proci.2010.06.024

[14] Kyoung Doo, K., and Sang Hee, H., "Arc Plasma Jets of a Nontransferred Plasma Torch," *IEEE Transactions on Plasma Science*, Vol. 24, No. 1, Feb. 1996, pp. 89–90. https://doi.org/10.1109/27.491705

[15] Sun, W., Won, S. H., Ombrello, T., Carter, C., and Ju, Y., "Direct Ignition and S-Curve Transition by In Situ Nano-Second Pulsed Discharge in Methane/Oxygen/Helium Counterflow Flame," *Proceedings of the Combustion Institute*, Vol. 34, No. 1, 2013, pp. 847–855. https://doi.org/10.1016/j.proci.2012.06.104

[16] Gao, J., Kong, C., Zhu, J., Ehn, A., Hurtig, T., Tang, Y., Chen, S., Aldén, M., and Li, Z., "Visualization of Instantaneous Structure and Dynamics of Large-Scale Turbulent Flames Stabilized by a Gliding Arc Discharge," *Proceedings of the Combustion Institute*, Vol. 37, No. 4, 2019, pp. 5629–5636. https://doi.org/10.1016/j.proci.2018.06.030

[17] Thelen, B. C., Chun, D., Toulson, E., and Lee, T., "A Study of an Energetically Enhanced Plasma Ignition System for Internal Combustion Engines," *IEEE Transactions on Plasma Science*, Vol. 41, No. 12, Dec. 2013, pp. 3223–3232. https://doi.org/10.1109/TPS.2013.2288204

[18] Galley, D., Pilla, G., Lacoste, D., Ducruix, S., Laux, C., Lacas, F., and Veynante, D., "Plasma-Enhanced Combustion of a Lean Premixed Air-Propane Turbulent Flame Using a Nanosecond Repetitively Pulsed Plasma," *43rd AIAA Aerospace Sciences Meeting and Exhibit*, AIAA Paper 2005-1193, 2005. https://doi.org/10.2514/6.2005-1193

[19] Zhu, J., Ehn, A., Gao, J., Kong, C., Aldén, M., Salewski, M., Leipold, F., Kusano, Y., and Li, Z., "Translational, Rotational, Vibrational and Electron Temperatures of a Gliding Arc Discharge," *Optics Express*, Vol. 25, No. 17, 2017, pp. 20243–20257. https://doi.org/10.1364/OE.25.020243

[20] Zhu, J., Sun, Z., Li, Z., Ehn, A., Aldén, M., Salewski, M., Leipold, F., and Kusano, Y., "Dynamics, OH Distributions and UV Emission of a Gliding Arc at Various Flow-Rates Investigated by Optical Measurements," *Journal of Physics D: Applied Physics*, Vol. 47, 2014, Paper 295203. https://doi.org/10.1088/0022-3727/47/29/295203

[21] Kong, C., Li, Z., Aldén, M., and Ehn, A., "Stabilization of a Turbulent Premixed Flame by a Plasma Filament," *Combustion and Flame*, Vol. 208, Oct. 2019, pp. 79–85. https://doi.org/10.1016/j.combustflame.2019.07.002

[22] Chen, W., Jin, D., Cui, W., and Huang, S., "Characteristics of Gliding Arc Plasma and Its Application in Swirl Flame Static Instability Control," *Processes*, Vol. 8, No. 6, 2020, p. 684. https://doi.org/10.3390/pr8060684

[23] He, L., Chen, Y., Deng, J., Lei, J., Fei, L., and Liu, P., "Experimental Study of Rotating Gliding Arc Discharge Plasma-Assisted Combustion in an Aero-Engine Combustion Chamber," *Chinese Journal of Aeronautics*, Vol. 32, No. 2, Feb. 2019, pp. 337–346. https://doi.org/10.1016/j.cja.2018.12.014

[24] Sun, J., Tang, Y., and Li, S., "Plasma-Assisted Stabilization of Premixed Swirl Flames by Gliding Arc Discharges," *Proceedings of the Combustion Institute*, Vol. 38, No. 4, 2021, pp. 6733–6741. https://doi.org/10.1016/j.proci.2020.06.223.

[25] Barbosa, S., Pilla, G., Lacoste, D., Scouflaire, P., Ducruix, S., Laux, C. O., and Veynante, D., "Influence of Nanosecond Repetitively Pulsed Discharges on the Stability of a Swirled Propane/Air Burner Representative of an Aeronautical Combustor," *Philosophical Transactions of the Royal Society A: Mathematical, Physical and Engineering Sciences*, Vol. 373, No. 2048, 2015, Paper 20140335. https://doi.org/10.1098/rsta.2014.0335

[26] Shcherbanev, S., Morinière, T., Solana-Pérez, R., Weilenmann, M., Xiong, Y., Doll, U., and Noiray, N., "Anchoring of Premixed Jet Flames in Vitiated Crossflow with Pulsed Nanosecond Spark Discharge," *Applications in Energy and Combustion Science*, Vol. 1, 2020, Paper 100010. https://doi.org/10.1016/j.jaecs.2020.100010

[27] Kundu, A., Klingmann, J., Whiddon, R., Subash, A. A., and Collin, R., "Operability and Performance of Central (Pilot) Stage of an Industrial Prototype Burner," *Proceedings of the ASME 2015 Power Conference Collocated with the ASME 2015 9th International Conference on Energy Sustainability, the ASME 2015 13th International Conference on Fuel Cell Science, Engineering and Technology, and the ASME 2015 Nuclear Forum, ASME 2015 Power Conference*, ASME, New York, June 2015. https://doi.org/10.1115/POWER2015-49449

[28] Subash, A. A., Whiddon, R., Collin, R., Aldén, M., Kundu, A., and Klingmann, J., "Flame Investigation of a Gas Turbine Central Pilot Body Burner at Atmospheric Pressure Conditions Using OH PLIF and High-Speed Flame Chemiluminescence Imaging," *Proceedings of the ASME 2015 Gas Turbine India Conference, ASME 2015 Gas Turbine India Conference*, ASME Paper V001T03A001, New York, Dec. 2015. https://doi.org/10.1115/GTINDIA2015-1212

[29] Subash, A. A., Collin, R., Aldén, M., Kundu, A., and Klingmann, J., "Laser-Based Investigation on a Dry Low Emission Industrial Prototype Burner at Atmospheric Pressure Conditions," *Proceedings of the ASME Turbo Expo 2016: Turbomachinery Technical Conference and Exposition*, Vol. 4B, ASME Paper V04BT04A005, New York, June 2016. https://doi.org/10.1115/GT2016-57242

[30] Döbbeling, K., Hellat, J., and Koch, H., "25 Years of BBC/ABB/ALSTOM Lean Premix Combustion Technologies," *ASME Journal of Engine Gas Turbines Power*, Vol. 129, No. 1, Jan. 2007, pp. 2–12. https://doi.org/10.1115/GT2005-68269

[31] Subash, A., *Laser-Based Investigations of Combustion Phenomena in Gas Turbine Related Burners*, Dept. of Physics, Lund University, Lund, Sweden, 2018, pp. 36–38.

[32] Sigfrid, I. R., Whiddon, R., Aldèn, M., and Klingmann, J., "Experimental Investigations of Lean Stability Limits of a Prototype Syngas Burner for Low Calorific Value Gases," *Proceedings of the ASME 2011 Turbo Expo: Turbine Technical Conference and Exposition*, Vol. 2, ASME, New York, June 2011, pp. 651–658. https://doi.org/10.1115/GT2011-45694

[33] Kundu, A., Klingmann, J., Subash, A., and Collin, R., "Flame Stabilization and Emission Characteristics of a Prototype Gas Turbine Burner at Atmospheric Conditions," *Proceedings of the ASME Turbo Expo 2016: Turbomachinery Technical Conference and Exposition*, Vol. 4B, ASME Paper V04BT04A011, New York, June 2016. https://doi.org/10.1115/GT2016-57336

[34] Kundu, A., Klingmann, J., Subash, A. A., and Collin, R., "Pilot-Pilot Interaction Effects on a Prototype DLE Gas Turbine Burner Combustion," *Proceedings of the ASME Turbo Expo 2016: Turbomachinery Technical Conference and Exposition*, Vol. 4B, ASME Paper V04BT04A012, New York, June 2016. https://doi.org/10.1115/GT2016-57338

[35] Gupta, A. K., Lilley, D. G., and Syred, N., *Swirl Flows*, Univ. of Michigan, Abacus Press, 1984, pp. 1–6. https://doi.org/10.1016/0010-2180(86)90133-1

[36] Andersen, B. W., and Binder, R. C., "The Analysis and Design of Pneumatic Systems," *Journal of Applied Mechanics*, Vol. 34, No. 4, 1967, pp. 1055–1055. https://doi.org/10.1115/1.3607835

[37] Kong, C., Gao, J., Zhu, J., Ehn, A., Aldén, M., and Li, Z., "Effect of Turbulent Flow on an Atmospheric-Pressure AC Powered Gliding Arc Discharge," *Journal of Applied Physics*, Vol. 123, No. 22, 2018, Paper 223302. https://doi.org/10.1063/1.5026703

[38] Kundu, A., Klingmann, J., Subash, A., and Collin, R., "Fuel Flexibility of a Multi-Staged Prototype Gas Turbine Burner," *Proceedings of the ASME Turbo Expo 2017: Turbomachinery Technical Conference and Exposition*, Vol. 4B, ASME Paper V04BT04A042, New York, June 2017. https://doi.org/10.1115/GT2017-64782

[39] Subash, A. A., Collin, R., Aldén, M., Kundu, A., and Klingmann, J., "Investigation of Hydrogen Enriched Methane Flame in a Dry Low Emission Industrial Prototype Burner at Atmospheric Pressure Conditions," *Proceedings of the ASME Turbo Expo 2017: Turbomachinery Technical Conference and Exposition*, Vol. 4A, ASME Paper V04AT04A056, New York, June 2017. https://doi.org/10.1115/GT2017-63924

[40] Turns, S. R., "An Introduction to Combustion: Concepts and Applications," Vol. 287, McGraw-Hill Companies, Rept. 0072300965, New York, 1996.

[41] Vervloessem, E., Aghaei, M., Jardali, F., Hafezkhiabani, N., and Bogaerts, A., "Plasma-Based N2 Fixation into NOx: Insights from Modeling toward Optimum Yields and Energy Costs in a Gliding Arc Plasmatron," *ACS Sustainable Chemistry & Engineering*, Vol. 8, No. 26, 2020, pp. 9711–9720. https://doi.org/10.1021/acssuschemeng.0c01815

[42] Subash, A. A., Collin, R., Aldén, M., Kundu, A., and Klingmann, J., "Experimental Investigation of the Influence of Burner Geometry on Flame Characteristics at a Dry Low Emission Industrial Prototype Burner at Atmospheric Pressure Conditions," *Proceedings of the ASME Turbo Expo 2017: Turbomachinery Technical Conference and Exposition*, Vol. 4A, ASME Paper V04AT04A058, New York, June 2017. https://doi.org/10.1115/GT2017-63950

Y. Ju
Associate Editor